Aquatic Toxicology 284 (2025) 107404

Contents lists available at ScienceDirect

Aquatic Toxicology

journal homepage: www.elsevier.com/locate/aqtox

Chronic tributyltin exposure induces metabolic disruption in an invertebrate model animal, *Lymnaea stagnalis*

István Fodor [a,b,*], János Schmidt [c], Réka Svigruha [a,b], Zita László [a,b], László Molnár [a,b], Sándor Gonda [a,d,e,f], Károly Elekes [a], Zsolt Pirger [a,b]

[a] Ecophysiological and Environmental Toxicological Research Group, HUN-REN Balaton Limnological Research Institute, 8237, Tihany, Hungary
[b] National Laboratory for Water Science and Water Security, HUN-REN Balaton Limnological Research Institute, 8237, Tihany, Hungary
[c] Institute of Biochemistry and Medical Chemistry, Medical School, University of Pécs, 7624, Pécs, Hungary
[d] Department of Pharmacognosy, University of Debrecen, 4002, Debrecen, Hungary
[e] Department of Botany, University of Debrecen, 4032, Debrecen, Hungary
[f] Institute of Environmental Science, University of Nyíregyháza, 4400, Nyíregyháza, Hungary

ARTICLE INFO

Keywords:
Tributyltin
Lymnaea stagnalis
Behavior
Histochemistry
Lipid metabolism
HSD17B12

ABSTRACT

Over the last 20 years, tributyltin (TBT) has been reported to cause metabolic disruption in both invertebrates and vertebrates, highlighting the need for further detailed analysis of its physiological effects. This study aimed to investigate the metabolic-disrupting effects of TBT from the behavioral to the molecular level. Adult specimens of the great pond snail (*Lymnaea stagnalis*) were exposed to an environmentally relevant concentration (100 ng L^{-1}) of TBT for 21 days. After the chronic exposure, behavioral alterations as well as histological, cellular, and molecular changes were investigated in the central nervous system, kidney, and hepatopancreas. TBT exposure significantly decreased feeding activity, while locomotor activity remained unchanged. At the histological level, the cellular localization of tin was demonstrated in all tissues investigated and, in addition, characteristic morphological changes were observed in the kidney and hepatopancreas. Tissue-specific changes in lipid profiles confirmed TBT-induced disruption of lipid homeostasis in mollusks, characterized by a consistent reduction in the proportion of polyunsaturated fatty acids and a shift toward more saturated lipids. The expression of 17β-hydroxysteroid dehydrogenase type 12 (HSD17B12) enzyme, involved in lipid metabolism in vertebrates, was reduced in all three tissues after TBT exposure. Our results show that TBT induces significant multi-level metabolic changes in *Lymnaea*, including direct alterations in feeding activity and lipid composition. Our findings also suggest that HSD17B12 enzyme plays a key role in lipid metabolism in mollusks, as in mammals, and is likely involved in TBT-induced metabolic disruption. Overall, our study extends the findings of previous studies on mollusks by providing novel behavioral as well as tissue-specific histological and metabolic data and highlights the complexity and evolutionary conserved way of TBT-induced metabolic disruption.

1. Introduction

Pollution by tributyltin (TBT), the biocide component of antifouling paints, has been one of the major threats to aquatic ecosystems for decades due to its rapid accumulation and high toxicity to a wide range of non-target animals including mollusks (reviewed by Beyer et al., 2022; Graceli et al., 2013; Lagadic et al., 2018; Scott, 2013). TBT-evoked endocrine disruption has a long history among the studies related to molluscan ecotoxicology (reviewed by Horiguchi and Ohta, 2020; Scott, 2013). Previous studies on mollusks mainly investigated the imposex-inducing effect of TBT with the underlying mechanisms (Graceli et al., 2013; Scott, 2013), revealing the interaction with the Retinoid X Receptor (Castro et al., 2007; Horiguchi et al., 2008; Lima et al., 2011; Nishikawa et al., 2004; Sternberg et al., 2008).

Later, studies reported that TBT can cause not only endocrine but also metabolic disruption (i.e. altered lipid homeostasis) in gastropods (Capitao et al., 2021; Janer et al., 2007). The same "obesogenic" effect of TBT has also been described in crustaceans (Jordao et al., 2015), echinoderms (Capitao et al., 2020), tunicates (Puccia et al., 2005), fish (Barbos et al., 2019; Kopp et al., 2017; Lyssimachou et al., 2015; Ortiz-Villanueva et al., 2018), and mice (Grun et al., 2006; Zuo et al., 2011). Some molecular aspects of the altered lipid metabolism of

* Corresponding author.
E-mail address: fodor.istvan@blki.hu (I. Fodor).

https://doi.org/10.1016/j.aquatox.2025.107404
Received 6 December 2024; Received in revised form 6 May 2025; Accepted 8 May 2025
Available online 9 May 2025
0166-445X/© 2025 The Author(s). Published by Elsevier B.V. This is an open access article under the CC BY license (http://creativecommons.org/licenses/by/4.0/).

gastropods were also investigated (Capitao et al., 2021; Lima et al., 2013). The findings of these studies suggested that 17β-hydroxysteroid dehydrogenase type 12 (HSD17B12), known to be essential for fatty acid synthesis and lipid metabolism in mammals (Heikelä et al., 2020), played a key role in TBT-evoked metabolic disruption (Lima et al., 2013). Moreover, TBT has been shown to interact with the peroxisome proliferator-activated receptor/RXR heterodimer of gastropods, which modulates the expression of genes involved in lipid homeostasis of echinoderms and vertebrates (Capitao et al., 2021). Recently, TBT was also demonstrated to alter embryonic and adult behaviors, such as feeding and locomotion, of molluscan (Jiang et al., 2023; Svigruha et al., 2024) and vertebrate species (Liang et al., 2017; Ponti et al., 2023; Zhang et al., 2016). Based on these findings, further and more detailed analyses were clearly needed to better understand the multifaceted physiological changes induced by TBT in aquatic animals.

Therefore, the aim of the present study was to investigate the metabolic-disrupting effects of TBT in the great pond snail (*Lymnaea stagnalis*). *Lymnaea* has been a widely used model in neuroscience, neuroendocrinology, and ecotoxicology for decades (reviewed by Amorim et al., 2019; Fodor et al., 2020; Rivi et al., 2020). Moreover, *Lymnaea* has also been a subject of TBT-induced endocrine disruption research for many years (Bandow and Weltje, 2012; Czech et al., 2001; Giusti et al., 2013a; Giusti et al., 2013b; Giusti et al., 2013c; Leung et al., 2007; Reátegui-Zirena and Salice, 2018; Svigruha et al., 2024). Given that TBT-based antifouling products are still available on the market contributing to the fresh supply of TBT pollution reported worldwide (Uc-Peraza et al., 2022), studies on TBT remain highly relevant and may have broad and important implications even today. To accomplish our aim, adult specimens of *Lymnaea* were exposed to 100 ng L^{-1} TBT for 21 days. After the chronic exposure, behavioral (feeding, locomotion) alterations as well as histological (tin accumulation, morphology), cellular (lipid composition), and molecular (HSD17B12 expression) changes were investigated in the central nervous system (CNS), kidney, and hepatopancreas ('digestive gland').

2. Materials and methods

2.1. Chemicals for chronic exposure

TBT chloride (TBT Cl) standard (#T50202-5G, Merck, Germany) was used for the treatments. First, a 1 mg mL^{-1} stock solution was prepared in dimethyl sulfoxide (DMSO, #D8418-100ML, Merck). The choice of DMSO as a carrier solvent was based on previous ecotoxicological studies performed on mollusks (Capitao et al., 2021; Lima et al., 2011; Lima et al., 2013; Svigruha et al., 2024). From this stock solution, 244 μg mL^{-1} working solutions were prepared weekly for the chronic exposure.

2.2. Experimental animals

5-month-old adult specimens of *Lymnaea* (with a shell length of 2.5–3.0 cm) were obtained from our laboratory-bred stocks. Snails were maintained in large plastic tanks containing 10L oxygenated artificial snail water (composition in mM: 0.1309 $NaHCO_3$, 0.0378 K_2SO_4, 0.4013 $CaCl_2 2H_2O$, 0.0390 $Mg(NO_3)2 \cdot 6H_2O$; pH=7.6) at 20°C (±1°C) on a 12:12 h light:dark regime with natural wavelength light. Specimens were fed on lettuce *ad libitum* two times a week.

2.3. Chronic exposure

The exposure settings followed the description of previous studies (Capitao et al., 2021; Lima et al., 2011; Lima et al., 2013). *Lymnaea* specimens were randomly selected from our laboratory-bred stocks and divided into two experimental groups as follows: 1) control group and 2) TBT-treated group (n = 30 animals/group). Each treatment was set up in three replicates, resulting in n=180 animals in total.

Animals of the control group were placed into tanks (n = 30 animals/tank) containing 10 L artificial snail water without DMSO. Animals of the TBT-treated group were also placed into tanks (n = 30 animals/tank) containing 10 L artificial snail water with 244 ng L^{-1} TBT Cl, which was equivalent to 100 ng L^{-1} TBT Sn. This exposure concentration was chosen for two main reasons. First, to ensure high compatibility with existing literature, as the same concentration has been used in a number of previous ecotoxicological studies on different mollusks, including *Lymnaea* (e.g., Bandow and Weltje, 2012; Capitao et al., 2021; Iyapparaj et al., 2013; Leung et al., 2007; Lima et al., 2011; Lima et al., 2013; Svigruha et al., 2024). Second, because this concentration is considered environmentally relevant (Antizar-Ladislao, 2008). The final DMSO concentration was ≤ 0.0001 % in the tanks of the TBT-treated group. The chronic exposure lasted for 21 days. During TBT exposure, the maintaining conditions (e.g., temperature and light) were the same as in the case of the laboratory-bred stocks. During the 21-day treatments, the animals were fed two times a week, with an equal amount of lettuce (3.5 g/individual), as also prescribed in OECD. In our preliminary experiment, DMSO at this ≤ 0.0001 % concentration after a 21-day exposure had no effect on feeding and locomotion of *Lymnaea* (**Supplementary Figure 1**).

Since a static exposure system was applied, the artificial water was completely changed every third day in both control and treated tanks, and TBT Cl was added again to maintain the 100 ng L^{-1} concentration. Recovery measurements were not performed since TBT is known to be stable in water (Bandow and Weltje, 2012; Inoue et al., 2006), hence a possible change of the nominal concentration due to degradation could be neglected. Consequently, we assumed that the approx. 100 ng L^{-1} nominal concentration was continuously maintained. Since TBT is known to tend to adsorb to plastics and glass, the tanks were equilibrated to TBT for one week before the start of the exposure.

2.4. Behavior tests

After the 21-day exposure, the feeding and locomotor activities were investigated according to the description of previous studies (Fodor et al., 2021; Pirger et al., 2021; Svigruha et al., 2021).

Feeding behavior (i.e. number of rasps) was followed by placing the snails from the control and TBT-treated groups (n=38 animals/group) individually into a Petri dish filled with 90 mL artificial snail water. Specimens were food-deprived for two days before the test. After accommodation for 10 min, 5 mL artificial snail water was added to the Petri dish and the number of spontaneous rasping activity was counted for 2 min. After this, 5 mL 20% sucrose solution was added to the Petri dish, which evokes feeding activity (rhythmic opening/closing of the mouth), and then the evoked feeding rate was counted for 2 min. The final feeding scores were obtained by subtracting the number of bites in response to artificial snail water from the number of bites performed in response to sucrose.

Locomotion (i.e. sliding) was followed by placing the snails both from control and TBT-treated groups into experimental tanks (10 × 20 × 3 cm). After accommodation for 10 min, the locomotor activity of the individual snails was recorded for 4 min with a German C-mount camera (#VE10320; Loligo Systems). The records were analyzed with the EthoVision XT 17.5 software (Noldus, the Netherlands) which plotted the trajectories and calculated the total distance covered by each individual snail.

2.5. Histochemical localization of tin and histological changes

After the 21-day TBT exposure, 15 animals were randomly selected from both control and TBT-treated groups. The CNS, kidney, and hepatopancreas were dissected from the animals and processed for histochemistry.

Tin distribution was visualized by a modified Timm's sulphide silver reaction (Geyer, 1973). The tissues were fixed in 4% paraformaldehyde dissolved in 0.1 M phosphate buffer (PB, pH=7.6) for 24 h at room

temperature, then washed thoroughly (6 × 15 min) in PB (0.1 M, pH=7.6), and cryoprotected in 20% sucrose solution. After this, the samples were embedded into Cryomatrix (#6769006, Thermo Fisher Scientific) and a series of alternating cryostat sections (15 μm) were mounted onto Superfrost ultra plus slides (#J3800AMNZ, Thermo Fisher Scientific). Next, the samples were incubated in a freshly prepared mixture of Na_2S (1.17 g) and $NaH_2PO_4 \bullet H_2O$ (1.19 g) dissolved in distilled water (pH=7.6) at room temperature for 30 mins. After thorough washing in several changes of PB for 48 h, the samples were incubated in a freshly prepared mixture of 10 mL gum Arabic 20%, 2 mL of a solution consisting of 2% hydroquinone, 5% citric acid, and 0.2 mL silver nitrate 10%. The development of the reaction was monitored under a stereomicroscope.

For histological investigations, the tissues were fixed in a freshly prepared formaldehyde-acetic acid fixative (6 mL conc. formaldehyde, 1 mL conc. acetic acid, and 18 mL distilled water) for 48 h at room temperature. After washing thoroughly in 0.1 M PB (pH=7.2), the fixed tissues were immersed in 20% sucrose solution for 1 h and then in 30% sucrose solution overnight at room temperature. Thereafter, the samples were embedded into Cryomatrix. Finally, a series of 15 μm thin alternating cryostat sections were mounted onto Superfrost ultra plus slides and stained with haematoxylin and eosin Y (H&E) following the standard protocol.

All sections were investigated in a Zeiss Axioplan microscope using bright-field for Timm's reaction or fluorescent illumination for H&E staining, using FITC filter cube according to the suggestion of (Ali et al., 2017).

2.6. Lipid extraction and LC-MS analysis

After the 21-day exposure, 30 animals (10 animals/replicate) were randomly selected from both control and TBT-treated groups for untargeted lipidomics analysis. The CNS, kidney, and hepatopancreas were dissected from the animals. Tissue samples were pooled in each replicate and their mass was measured (**Supplementary Table 1**). Lipid extraction followed the original method developed by (Bligh and Dyer, 1959). Briefly, samples were homogenized in a chloroform-methanol mixture 1:2 (v/v). To standardize extraction efficiency, the solvent was added to the samples proportional to tissue mass at a ratio of 1:20. After homogenization, ultrasonic extraction was performed. Following vortexing, chloroform and water were added to achieve a chloroform/methanol/water composition of 2:2:1.8 (v/v/v). After additional vortexing, samples were centrifuged at 12,000 g for 10 minutes at 18°C. The lipid-containing lower phase was manually separated and evaporated under nitrogen gas. Lipids were subsequently re-dissolved in methanol, and samples were normalized based on their initial masses.

Chromatographic separation was performed using a Thermo Ultimate 3000 UHPLC™ system (Thermo Fisher Scientific) with a Kinetex C18 reversed-phase column (2.6 μm, 2.1 mm × 150 mm i.d.; Phenomenex; USA). For the multistep gradient-based separation method, we utilized two different solvents. Solvent A consisted of water/formic acid (99.9/0.1, v/v), while solvent B was composed of water/formic acid/methanol (9.9/0.1/90, v/v/v). Both eluents were supplemented with 10 mM ammonium formate. The gradient program included the following steps: from 0 to 1.0 minutes, the composition was 20% B; from 1.0 to 10.0 minutes, it increased from 20.0% to 80.0% B; from 10.0 to 22.0 minutes, it increased from 80.0% to 100.0% B and remained at 100% B until 40.0 minutes; then, from 40.0 to 41.0 minutes, the composition decreased from 100.0% to 20.0% B, followed by a 6-minute equilibration of the column. The flow rate was 300 μL min^{-1}. Data-dependent mass spectrometric acquisition was performed with a Bruker Maxis 4G UHR-QTOF instrument (Bruker Daltonics, Germany). The mass spectrometer was operated in positive ion mode, and the scanning range was set to 100–1200 m/z. The flow of nebulizer gas was 10 L min^{-1} at a pressure of 2.5 bar, and the temperature was set at 220°C. The capillary voltage was 3.8 kV.

The 25 most intensive compounds were selected for CID fragmentation. The collected data were converted to Abf format using the Reifycs file converter tool and processed with the MS-DIAL (Version 5.1.230222) software. For database identification, the MS-DIAL LipidBlast (version 68) MSP database was used (last edited on April 21st, 2022). The database identification was performed based on the suggestions of a previous study (Tsugawa et al., 2020): molecules were considered identified if their similarity (match) score exceeded the value of 1.2. A representative fragment spectrum-based identification is presented in **Supplementary Figure 2**.

2.7. In silico searches and bioinformatic analysis

The neural transcriptome data obtained in our previous work (Pirger et al., 2024) were used to identify the coding sequence of HSD17B12 in *Lymnaea* (Lym-HSD17B12). For homology-searching, relevant vertebrate and molluscan HSD17B12 sequences were used as search queries (**Supplementary Table 2**). We also compared the obtained sequence with the public *Lymnaea* CNS transcriptome shotgun assembly (sequence read archive: #DRR002012; (Sadamoto et al., 2012)). The identified sequence was submitted to the NCBI Nucleotide database (GenBank number: #PP400770).

Conserved domain search using NCBI CDD/SPARCLE (Lu et al., 2020; Marchler-Bauer et al., 2017) was first performed to check if the key regions were present in the deduced protein sequence. For 3D structure prediction, the computational modelling was made with AlphaFold2, a protein structure predicting algorithm (Jumper et al., 2021). The amino acid sequence was run through the GoogleColab platform (Bisong, 2019) followed by a further examination with PyMOL (PyMOL, 2020) and Swiss-PdbViewer 4.1.0 (Guex and Peitsch, 1997). For detailed sequence conservation analysis, Lym-HSD17B12 was aligned with chosen sequences from NCBI: *Nucella lapillus* HSD17B12 (#JX625140), *Haliotis diversicolor supertexta* HSD17B12 (#ADF80270), *Danio rerio* HSD17B12 (#ENSDARP00000014003), *Homo sapiens* HSD17B12 (#ENSP00000278353). The alignment was performed with EMML-EBI Multiple Sequence Alignment (https://www.ebi.ac.uk/Tools/msa/clustalo/) and highlighted using BOXSHADE (https://github.com/mdbaron42/pyBoxshade).

For phylogenetic analysis, the multiple sequence alignment used to generate the maximum likelihood tree consisted of 23 amino acid sequences (**Supplementary information**). The alignment was performed using the ClustalW function with BLOSUM62 substitution matrix in Molecular Evolutionary Genetics Analysis v7 software (Kumar et al., 2016). The alignment was then analysed to get the best fitting model, which was determined to be LG with gamma-distributed rates. Bootstrapping support for the tree was conducted with 1000 bootstrap replicates, the bootstrap values (%) are indicated at each branch point. All positions containing gaps and missing data were eliminated. There was a total of 261 positions in the final dataset.

2.8. Tissue distribution of Lym-HSD17B12 expression

The CNS, heart, kidney, and hepatopancreas were dissected from 5-month-old animals (n=5) obtained from our base laboratory-bred stocks. The respective tissues were pooled and homogenized in TRI reagent (#93289, Merck) with a TissueLyser LT device (Qiagen, Germany). RNA was isolated with the Direct-zol™ RNA MiniPrep kit (#R2050, Zymo Research). To ensure that the samples are free from genomic DNA contamination, an additional DNase treatment was also made with the TURBO DNA-free™ Kit (#AM1907, Thermo Fisher Scientific). The RNA was quantified by a NanoDrop One device (#ND-ONE-W, Thermo Fisher Scientific). The RevertAid H Minus First Strand cDNA Synthesis Kit (#K1631, Thermo Fisher Scientific) was used for reverse transcription (RT), applying random hexamer primers and 300 ng from all RNA samples.

PCR primers were designed for the identified coding region of

HSD17B12 with the SnapGene Viewer software (GSL Biotech, v4.1.7). The applied primer set was as follows: the forward primer for HSD17B12: 5′ – CTT GCA GCC AAA GGC CTT AAT GTT G – 3′; the reverse primer for HSD17B12: 5′ – ACA TTG TTG ACC AGG ACT CCG ATG – 3′ (Integrated DNA Technologies, Belgium). As a control to ensure the quality of reverse transcription, actin was also amplified for all examined tissues. The applied primer set for actin was as follows: the forward primer: 5′ – TCC CTT GAG AAG AGC TAC GAG C – 3′; and the reverse primer: 5′ – GAG TTG TAG GTG GTT TCG TGG – 3′ (Integrated DNA Technologies). The PCR reaction was performed in 20 μL reaction volume at 95°C for 4 min followed by 35 cycles of 95°C for 30 s, 56°C for 30 s and 72°C for 10 s by a T1 Thermocycler PCR device (Biometra, Germany).

2.9. qRT-PCR measurement of Lym-HSD17B12 expression

After the 21-day TBT exposure, 12 animals were randomly selected from the control and TBT-treated groups (i.e. 4 animals/replicate/group). The CNS, kidney, and hepatopancreas were prepared from the animals. From the individual tissue samples, RNA isolation, additional DNase treatment, and reverse transcription with 200 ng RNA for all samples were performed as described above.

To quantify the change of mRNA expression level of Lym-HSD17B12, qRT-PCR was performed. Each 20 μL reaction volume contained 10 μL 2x SYBR Green PCR Master Mix (#208252, Qiagen), 6 μL distilled water, 2 μL cDNA sample (20 ng), and 1 μL for each primer (500 nM final concentration). Following the method of previous studies performed on *Lymnaea* (Batabyal et al., 2024; Rivi et al., 2022; Rivi et al., 2023), elongation factor 1α (EF1α) and β-tubulin (βTUB) were used as housekeeping genes. The applied primer sets were as follows: forward for EF1α: 5′ – GTG TAA GCA GCC CTC GAA CT – 3′; reverse primer for EF1α: 5′ – TTC GCT CAT CAA TAC CAC CA – 3′; forward for βTUB: 5′ – GAA ATA GCA CCG CCA TCC – 3′; reverse for βTUB: 5′ – CGC CTC TGT GAA CTC CAT CT – 3′ (Integrated DNA Technologies). Each preparation of Lym-HSD17B12, EF1α, and βTUB was added to 96-well plates in triplicates. The reaction was performed at 95°C for 2 min followed by 40 cycles of 95°C for 5 s, 60°C for 30 s using the QIAquant 96 2plex device (Qiagen) with the Q-Rex software (v. 2.0).

At the end of the measurement, a melting curve analysis was performed (plate read every 0.3°C from 60 to 95°C) to determine the formation of the specific products. The amplification efficiency of the primer pairs calculated from the standard curves was within the desired range of 95%–105% (Lym-HSD17B12: 101%; EF1α: 98%, βTUB: 100%). Changes in Lym-HSD17B12 mRNA expression, normalized to the arithmetic mean of the two reference genes, were calculated with the $2^{-\Delta\Delta Ct}$ method.

2.10. Statistical analysis

Statistical analysis of data obtained during the behavior and qRT-PCR experiments was made with the OriginPro 2018 software (OriginLab Corp., USA). The normality of the datasets was investigated using the Shapiro-Wilk test and the homogeneity of variances between groups was checked with the Levene-test. The feeding and locomotor data were analyzed using the two-sample t-test. The qRT-PCR data were analyzed with the two-sample t-test or the Mann-Whitney test. In the case of lipidomics, the peak areas were used for relative quantification. Statistical analysis of data was made with the F-test built in the MS-DIAL software to assess differential changes between the samples (treated_vs_control; 1.5 fold change and 0.05 adjusted P value). Lipid annotations were processed using the lipidr package 2.15.1 (Mohamed and Jeffrey, 2023) in R 4.5.0 (Team, 2025) to yield numeric data on saturation and average fatty acid chain length. In brief, the fold-change values of individual phosphatidylcholines (PCs), ether-phosphatidylcholines (EtherPCs) and other less abundant lipids were sought for differential change patterns in the dataset. Only lipids with annotations at the total chain length level were processed. Side chain length was defined as $Cn \leq 16$, short; $16 < Cn < 20$, medium; $Cn > 20$, long. Average saturation was defined as nbonds = 0, saturated (SAT); 0 < nbonds < 2, unsaturated (UNSAT); nbonds ≥ 2, polyunsaturated (PUFA).

3. Results and discussion

3.1. Feeding and locomotor activity

The effect of chronic TBT exposure on the feeding and locomotor activities of adult specimens of *Lymnaea* is shown in Fig. 1. Compared to the control, a 37.3% reduction in feeding score was observed in the TBT-treated group, indicating a significant reduction in feeding activity after exposure to TBT (t_{70} =5.09, $p < 0.001$) (Fig. 1**A**). In contrast, the TBT exposure did not alter locomotor activity (Fig. 1**B**), as no significant differences were detected in the total distance covered between the control and treated groups ($p > 0.05$). In accordance with the decreased feeding activity, the body weight of the snails in the treated group was significantly lower at the end of the treatment compared to that of the animals in the control group ($t_{38} = 2.22$, $p < 0.05$) (**Supplementary Figure 3**).

The current literature data on the effect of TBT on the feeding activity of different animals are contradictory. TBT as an obesogenic compound is known to increase the food intake (and body weight) of goldfish (Zhang et al., 2016), zebrafish (Lyssimachou et al., 2015), mice (Ponti et al., 2023), and rats (Rodrigues-Pereira et al., 2022) even at low concentrations. In contrast to vertebrates, after the application of 30, 60, or 120 ng L^{-1} TBT to embryos of the squid *Sepia pharaonic*, a significantly decreased feeding time and body weight of juveniles were reported in a recent study (Jiang et al., 2023). In our previous study, 100 ng L^{-1} TBT exposure during the entire embryogenesis was shown to decrease the feeding activity of *Lymnaea* embryos (Svigruha et al., 2024). In addition to studies performed on mollusks, to our best knowledge, there is only two invertebrate study investigating the effects of TBT on feeding behavior (Jordao et al., 2016; Ofoegbu et al., 2016). Acute (48 h) sub-lethal exposures with 16 and 103 ng L^{-1} TBT were shown to significantly reduce the feeding of the freshwater planarian *Schmidtea mediterranea* (Ofoegbu et al., 2016). Moreover, a 24 h-exposure to 10 nM TBT (appr. 3.2 ng L^{-1}) already decreased the feeding rate of the water flea, *Daphnia magna* (Jordao et al., 2016). The decreased feeding activity of adult *Lymnaea* specimens shown in the present study are consistent with the previous findings, suggesting that the effect of TBT on feeding is opposite to that described in vertebrates.

The current literature data on the effect of TBT on the locomotor activity of aquatic animals are controversial. In an earlier study on zebrafish embryos, a significantly reduced locomotor activity was reported following the application of 317 ng L^{-1} TBT for 96 h (Liang et al., 2017). In contrast, three-week-old hatchlings of rainbow trout exposed to 0.5 μg L^{-1} or 2.0 μg L^{-1} TBT for 21 days displayed a significantly increased swimming activity (Triebskorn et al., 1994). The swimming activity of juveniles of *S. pharaonis* significantly increased after the administration of 30 and 60 ng L^{-1} TBT during embryogenesis (Jiang et al., 2023). In our previous study, the locomotor (gliding) activity of *Lymnaea* embryos was not altered during the exposure to 100 ng L^{-1} TBT (Svigruha et al., 2024). Sub-lethal exposures (8, 16, and 103 ng L^{-1}) to TBT for 48 h were shown to reduce the locomotor activity of the planarian *S. mediterranea* (Ofoegbu et al., 2016). Based on these findings, the effect on locomotor activity seems to be species-specific. However, the different changes might also be explained by the not completely identical endpoints investigated and the different exposure and concentration conditions (acute vs. chronic, ng L^{-1} vs μg L^{-1}).

In earlier studies performed on vertebrates, TBT applied even at environmentally-relevant concentrations was demonstrated to cross the blood-brain barrier, induce neuroinflammation and oxidative stress, alter the chemical synaptic transmission, and change the level of

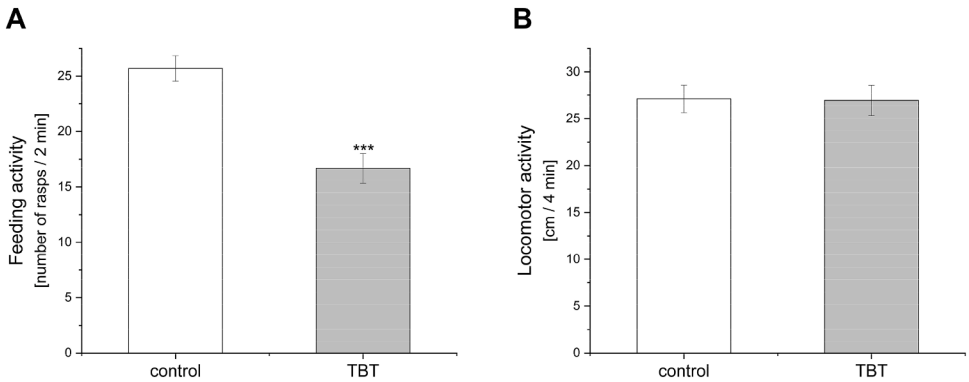

Fig. 1. Feeding (number of rasps/2 min) (**A**) and locomotor (distances covered/4 min) (**B**) activities of the experimental groups (control – white column; TBT-treated – grey column) of adult *Lymnaea* specimens after 21-day TBT exposure. The feeding activity of TBT-treated snails significantly decreased, while the locomotor activity did not change. Each bar represents mean ± SEM (n = 38 animals/group). Significant difference to the control is indicated by an asterisk (*$p < 0.05$).

different neurotransmitters (Kishimoto et al., 2001; Li and Li, 2021; Mitra et al., 2013; Yu et al., 2013). Some elements of the neuronal circuits which are responsible for the regulation of feeding behavior in mice have been investigated regarding the increased feeding activity evoked by TBT. Accordingly, a significant decrease in the immunoreactivity of the orexigenic Neuropeptide Y and the anorexigenic pro-opiomelanocortin in different parts of the feeding circuits was demonstrated (Bo et al., 2016; Farinetti et al., 2018; Ponti et al., 2023). From our side, future studies are aimed at investigating the neuronal mechanisms of the decreased feeding activity of *Lymnaea*. Since network functions, such as pattern generation, modulation, and motivational state regulation, involved in *Lymnaea* feeding behavior are well-known (reviewed by Benjamin and Crossley, 2020), this species provides an excellent opportunity to investigate the TBT-induced changes both at the level of neuronal circuits and individually identified neurons.

3.2. *Tin accumulation and histological changes in Lymnaea tissues*

A number of earlier studies has revealed the accumulation of TBT in the whole-body tissue of adult molluscan species using the standard gas chromatography or inductively coupled plasma mass spectrometry approaches (e.g., Chen et al., 2011; Inoue et al., 2004; Inoue et al., 2006; Martínez et al., 2017; Metelkova et al., 2022; Wang et al., 2010). However, these studies did not deal with the localization of tin. In a

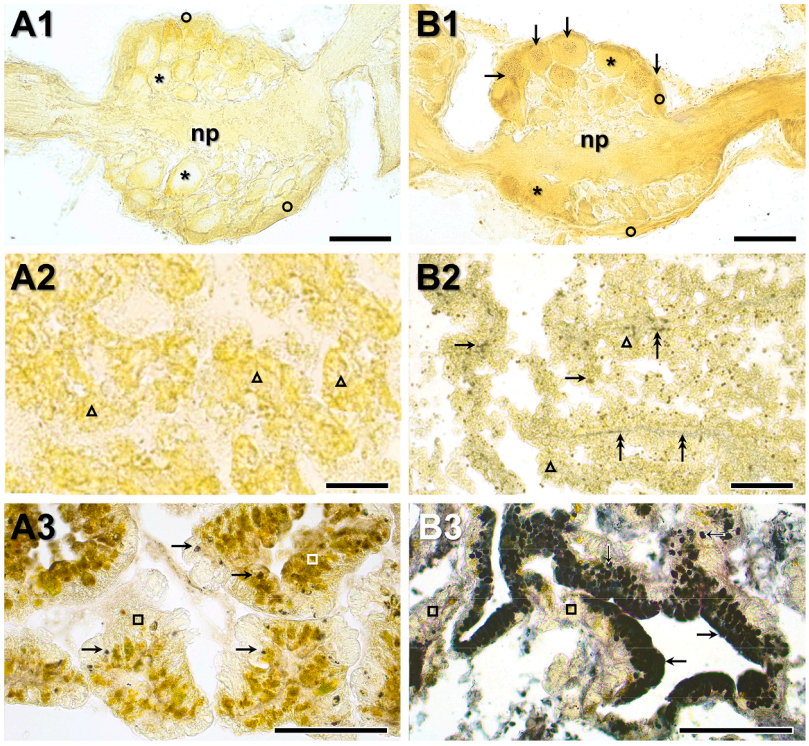

Fig. 2. Representative micrographs of the buccal ganglion (upper row), kidney (middle row), and hepatopancreas (i.e. digestive gland; lower row) taken from control (**A** column) and TBT-treated (**B** column) animals after 21-day TBT exposure. Timm's sulphid-silver reaction shows finely granulated black precipitations in the buccal ganglion (**B1**) and kidney (**B2**) of tin exposed animals but not in the controls (**A1** and **A2**). In the buccal ganglion, black precipitations (arrows) are located in the neural perikarya (asterisks), neuropil (np), and ganglion sheath (circles). In the kidney, fine black precipitations are seen both in cells (arrows) of the epithelium (triangles) and in the connective tissue septa (double arrows). The acinar epithelium (squares) of the hepatopancreas of both control (**A3**) and exposed (**B3**) animals displays several granular structures with variable size and content. Timm's reaction showssome granules containing only a few black grains (arrows) in the control sections, while intensely labelled granules (arrows) are seen in the epithelial cells of the TBT-treated samples. Bars = 25 μm.

pioneer study, the histopathological changes induced by long-term 100 ng L^{-1} TBT exposure were investigated in the albumen gland, dermis, foot, lung, mantle, and prostate gland of *Lymnaea,* revealing marked degenerative effects (tissue necrosis) and inflammatory responses in the epithelial tissue of the lung and foot (Czech et al., 2001). However, the possible histological changes in other tissues, including the CNS, kidney, and hepatopancreas, of *Lymnaea* have not yet been investigated. Keeping this in mind, in the present study, we investigated tin accumulation and histopathological effects of TBT in the CNS, kidney, and hepatopancreas of *Lymnaea*.

The accumulation of tin in the examined tissues is shown in Fig. 2. Compared to the control group (Fig. 2**A1-A3**), Timm's reaction produced finely granulated black precipitation in the neural perikarya, neuropil, and ganglion sheath of the CNS (Fig. 2**B1**), as well as in the epithelial cells and connective tissue septa of the kidney (Fig. 2**B2**), and in the epithelial cells of the hepatopancreas (Fig. 2**B3**) of TBT-exposed animals. The most intensive tin accumulation was observed in the epithelial cells of hepatopancreas. Similarly to our previous results obtained on *Lymnaea* embryos (Svigruha et al., 2024), the CNS also proved to be a potential target for tin accumulation in adults, although the tin reaction was significantly less intense than in the kidney and hepatopancreas. In the case of other metals (e.g., Al and Cd), after an initial systemic accumulation in *Lymnaea* tissues, redistribution into the digestive gland was detected where the intracellular lysosomal granules play a key role in metal sequestration (Desouky, 2006). We hypothesize that this is also the case for TBT, which is reflected by the highly intensive tin accumulation in the hepatopancreas. Importantly, this is the first study to demonstrate the cellular localization of tin in TBT-exposed adult specimens of a molluscan species. Of note, the applied histochemical reaction is not selective for tin since some heavy metals (e.g., cadmium, copper, zinc) also form precipitation with sulfide silver reaction, but significant occurrence of other heavy metals can be excluded in our experiments.

Further investigations with H&E staining after TBT exposure revealed remarkable morphological changes both in the kidney and hepatopancreas, but not in the CNS (Fig. 3). In the kidney sacs, the renal epithelium of the exposed animals became remarkably thinner (Fig. 3**B2**), while the connective tissue septa were thicker compared to that of the control (Fig. 3**A2**). Similarly, the epithelium of the digestive gland of TBT-treated snails was also thinned (Fig. 3**B3**) compared to the control (Fig. 3**A3**). Hypothetically, the observed changes can be the results of necrosis, but further investigations are needed to clear unequivocally this question. In recent studies, when applying TBT at mg kg^{-1} concentrations, the histopathological changes in the brain of mice and rats were shown to present remarkable morphological changes, such as disturbed cortical layers, were demonstrated (Sakr et al., 2021; Shaban et al., 2023). Moreover, a 4-week exposure of TBT (4.8 μg $snail^{-1}$) caused severe histopathological and ultrastructural alterations (e.g., hyperchromatic nuclei, atrophy of the perikarya of some neurons, increased number of autophagosomes) in the cerebral ganglia of the land snail, *Eobania vermiculata* (Essawy et al., 2011). We failed to observe similar alterations, suggesting that the applied 100 ng L^{-1} concentration was too low for destructive effects on the CNS. However, the chronic TBT exposure evoked notable degenerative effects in the epithelial tissue of both the kidney and hepatopancreas, which results are in line with the previous findings obtained on mollusks (Czech et al.,

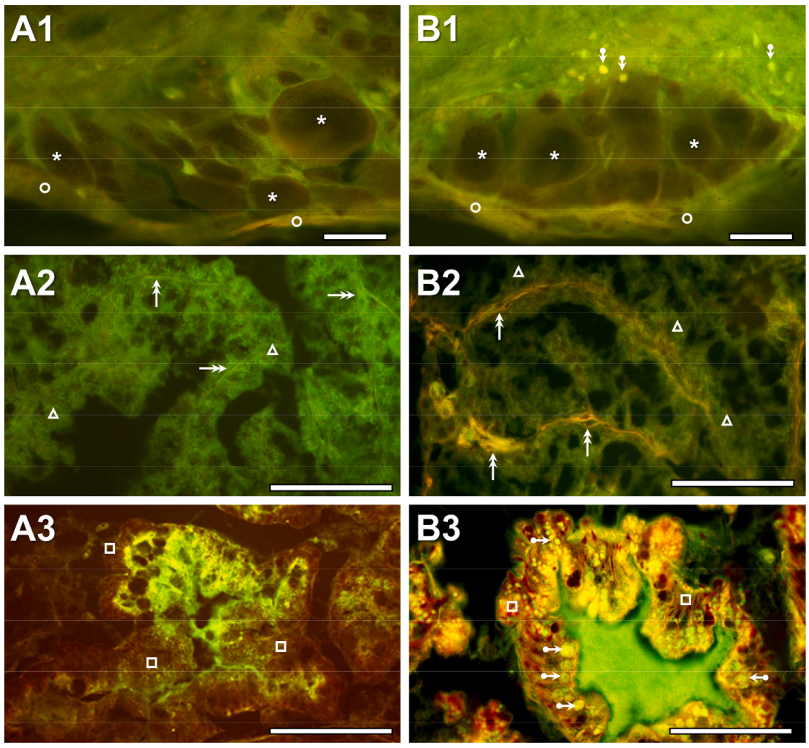

Fig. 3. Representative micrographs of the buccal ganglion (upper row), kidney (middle row), and hepatopancreas (i.e. digestive gland; lower row) taken from control (**A** column) and TBT-treated (**B** column) animals after 21-day TBT exposure. Following H&E staining and fluorescent illumination, characteristic histological differences between control and treated samples are seen. Compared to the control (**A1**), the presence of protein rich granules with variable fluorescent emission (bullet arrows) are seen in the neuropil of the buccal ganglion of treated snails (**B1**). Asterisks – nerve cell bodies; circle – ganglion sheath.The kidney of control animals displays regular, cuboidal epithelium (triangles) located on a connective tissue septum (double arrows) (**A2**). In contrast, TBT-exposure resulted in degeneration of the kidney epithelium (triangles) and swelling of the connective tissue septa (double arrows) (**B2**). Acinar epithelium (squares) of the hepatopancreas of both control (**A3**) and exposed (**B3**) animals had several granular structures with variable size and content. Note the similar pattern and size of protein rich granules (bullet arrows) and metal-accumulating granules (Fig. 2) in the acinar epithelium. Note bright fluorescence in the acinar lumen indicating an intense transportation of the granular proteins by exocytosis. Similar to the kidney, a thinned epithelium and a thicker connective tissue septa can be observed in the hepatopancreas of the exposed snails. Bars = 25 μm.

2001; Zhou et al., 2010) and fish (Fent and Meier, 1992; Rabitto et al., 2005).

Compared to the control (Fig. 3**A1**), accumulation of granules characterized by distinct fluorescent (from green to yellow) emissions wase seen in the neuropil of treated animals (Fig. 3**B1**). Since eosin is an effective stain of cationic proteins binding to their arginine, histidine, lysine, and tryptophan residues and it is also a pH indicator (Waheed et al., 2000), we suppose that these granules are protein-rich and represent distinct types of lysosomes. In the kidney of control snails, the epithelium was rich in secretory granules (Fig. 3**A2**), while the number of connective tissue cells and fibers increased significantly in the TBT-exposed animals (Fig. 3**B2**). Some of the connective tissue cells were tightly packed with granules, showing strong fluorescence. The structure of digestive gland of *Lymnaea* is well-known to consist of many tubules of digestive diverticula and the epithelium is composed of three main cell types: digestive, excretory, and thin cells (Desouky, 2006; Elangovan et al., 2000). The digestive cells contain three types (small, green, and yellow) of granules, which corresponds to different developmental stages of lysosomes with the yellow granules representing the mature ones (Desouky, 2006). In contrast to the control (Fig. 3**A3**), the number of excretion granules increased in the digestive gland cells of the TBT-treated animals which were also present in the lumen of the tubule (Fig. 3**B3**). Intracellular metal detoxification by lysosomal activity is well-known in animals. Previously, trace metals were demonstrated to increase the number of excretory/lysosomal granules in the kidney and hepatopancreas of *Lymnaea* (Desouky, 2006). Also, removal of TBT via digestive cell lysosomal compartment was shown in the Asian clam, *Corbicula fluminea* (Champeau and Narbonne, 2006). Moreover, in an earlier study on *Anodonta anatine*, the frequent localization of tin in the secondary or tertiary lysosomes of nephrocytes was demonstrated following the application of dibutyltin for months (Herwig and Holwerda, 1986). Based on these findings, we suppose that TBT increased the lysosomal activity in all *Lymnaea* tissues investigated, which is supported by the increased number of excreted granules.

3.3. Effect of TBT on lipid composition

As mentioned in the Introduction, TBT, as well as other organotins such as triphenyltin, were previously shown to alter the lipid homeostasis in mollusks (Capitao et al., 2021; Janer et al., 2007; Lyssimachou et al., 2009). However, these studies focused only on the gonads or the digestive gland/gonad complex. Moreover, these studies investigated only the changes in the total lipid amount and fatty acid composition without directly measuring the amount of different lipids. In order to provide further and possibly new insight into the TBT-evoked metabolic-disruption, we investigated the potential direct changes of the lipid content of the CNS, kidney, and hepatopancreas.

Using an untargeted lipidomics approach, 132, 178, and 222 lipid features in the CNS, kidney, and hepatopancreas, respectively, could be identified (**Supplementary Table 3-5**). From the identified lipids, the amount of 16 lipids in the CNS, the amount of 27 lipids in the kidney, and the amount of 30 lipids in the hepatopancreas changed significantly due to the chronic TBT exposure (Table 1). Since the different tissues have their own lipid fingerprint, the identified lipids showing significant changes were tissue dependent. As expected, more lipid composition change was detected in the kidney and hepatopancreas, since the metabolic rate of these organs is higher than that of the CNS. A preliminary functional analysis was also carried out to reveal deeper insights into the potential changes in the lipid homeostasis induced by TBT (Fig. 4). In the CNS, the treatment increased the proportion of several features with more saturated side chains, indicating a shift from PUFA to UNSAT ($p < 0.05$, $n = 22$) in the phospholipid class, but not across all lipid classes. No significant change was observed in chain length. In the kidney, no significant changes were determined. In the hepatopancreas, in contrast, the proportion of shorter-chain features increased, while the proportion of medium and long chains decreased, but this effect was only observed in the ether phospholipid class ($p = 0.022$), and not across all lipids ($p = 0.42$) or specifically within the phospholipid class ($p = 0.16$). Specifically, the $\log_2$FC values for short, medium, and long chains were 1.46 ± 1.15 ($n = 8$), -1.18 ± 2.28 ($n = 32$), and -1.03 ± 4.10 ($n = 3$), respectively. Additionally, the proportion of saturated chains also increased within the ether phospholipid class, at the expense of PUFA and UNSAT ($p = 0.0324$, $n = 43$), but this shift was not observed in all lipids or specifically in the PC class. Altogether, a shift from unsaturated to saturated lipids was observed in two organs, however with different outcomes – either an increase in the proportion of SAT or of mono-UNSAT. Moreover, different lipid classes were affected in each case. In the hepatopancreas, this shift is accompanied by a reduction in fatty acid chain length.

Table 1
Fold change values of the significantly changed lipids (treated_vs_control; 1.5 fold change and 0.05 adjusted P value) in the CNS, kidney, and hepatopancreas after the 21-day TBT exposure. Abbreviations: PC – phosphatidylcholine; LPC – lysophosphatidylcholine; PE –phosphatidylethanolamine; LPE – lysophosphatidylethanolamine; SM – sphingomyelin: SPB – sphingoid base; DG – diacylglycerol; CAR – acylcarnitine; ST – sterol.

CNS		Kidney		Hepatopancreas	
Lipid	FC value	Lipid	FC value	Lipid	FC value
PC(O-32:1)	-2.06	PC(38:3)	-61.97	PC(34:3)	4.43
PC(O-36:9)	-3.73	DG(34:0)	8.95	PC(O-37:7)	-5.8
PC(O-42:11)	2.59	PE(40:8)	9.98	LPC(O-18:0)	3.17
LPC(O-16:0)	-1.65	DG(24:3)	10.34	PC(27:0)	-2.67
PC(38:6)	-1.76	PC(O-39:4)	1.51	PC(32:3)	-4.15
PC(O-33:0)	-1.65	PC(O-33:2)	1.54	PC(O-39:5)	-2.68
PC(32:3)	1.68	PC(36:5)	1.51	PC(41:6)	-1.79
PC(36:1)	1.9	PC(O-32:0)	2.57	SPB(19:1;O2)	-2.54
PC(O-40:6)	-1.68	PC(O-33:1)	2.76	PC(O-42:2)	-5.58
PE(P-38:4)	-3.15	PC(O-38:3)	1.74	PC(42:6)	-2.39
LPE(O-16:1)	2.49	LPE(18:1)	1.72	SM(45:1;O2)	-63.8
PC(O-40:4)	-1.53	PC(42:5)	2.02	CAR(24:0)	-6.03
PC(O-30:0)	3.1	PC(36:3)	1.98	PC(O-40:4)	-1.52
PC(O-42:5)	-1.61	PC(38:2)	-1.98	PC(O-30:0)	2.77
SM(32:0;O2)	-1.73	PE(O-16:1)	2.23	PC(O-32:0)	1.57
PC(35:2)	3.82	DG(37:7)	-5.05	PC(36:3)	-2.39
		PC(O-36:2)	-1.57	LPC(O-20:1)	-2.01
		PC(38:1)	-1.57	LPC(20:1)	-4.73
		LPC(20:4)	-1.79	CAR(23:0)	-2.08
		PC(36:2)	-1.87	ST(28:2;O)	-2.26
		PC(O-31:0)	-3.17	PC(33:4)	-2.02
		PC(O-36:3)	-2.77	PC(40:9)	-3.77
		PC(O-36:4)	-2.7	PC(O-31:0)	2.33
		PC(35:1)	-2.23	LPC(O-15:0)	-2.43
		PC(O-36:5)	-2.2	PC(O-34:4)	1.66
		PC(32:3)	-2.48	PC(38:7)	-1.76
		LPC(18:3)	-2.36	PC(40:7)	-4.03
		PC(34:6)	-2.4	LPC(18:2)	-2.38
				CAR(22:0)	-7.93
				PC(36:5)	4.4

Our results confirmed the previous idea that untargeted LC-MS lipidomics is a powerful experimental approach to analyze the metabolic effects of TBT on aquatic invertebrates (Jafari et al., 2023). The first study investigating the potential effects of organotin compounds on lipid homeostasis in invertebrates was published by (Janer et al., 2007). In this pioneer work, when exposing specimens of the ramshorn snail *Marisa cornuarietis* to 30, 125, and 500 ng L^{-1} TBT, respectively, for 100 days, a significant increase in the fatty acid levels and percentage of lipids was detected in the digestive gland/gonad complex of females exposed to 500 ng L^{-1}. Moreover, fatty acid profiles were altered in both males and females exposed to 125 and 500 ng L^{-1} TBT depending on the saturation degree and carbon chain length. In another study on *M. cornuarietis*, alterations in the lipid content and fatty acid profiles were also reported following the application of triphenyltin at 30, 125, and 500 ng L^{-1} concentrations for 7 days (Lyssimachou et al., 2009). Comparing the findings of previous studies with the results of the present study, all evidence suggests that organotin compounds disrupt lipid

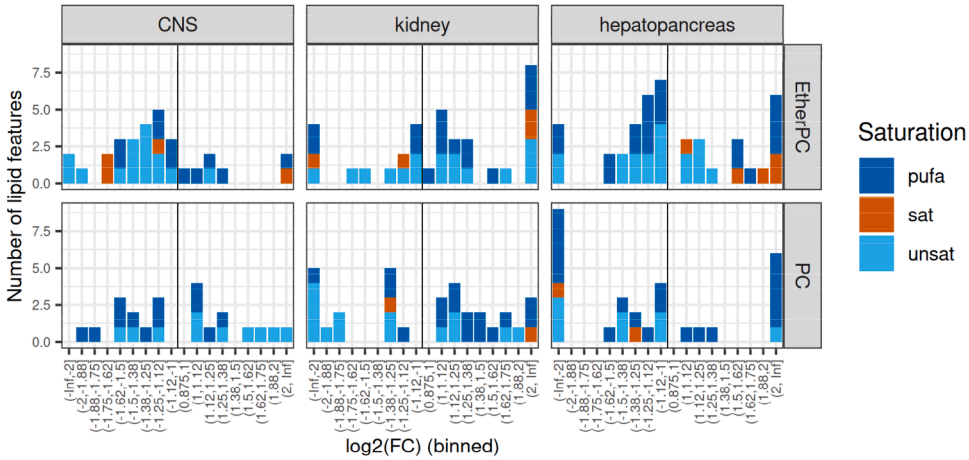

Fig. 4. Distribution of $\log_2$(fold-change) values of lipid features with MS/MS resolved side chains in various annotated lipid classes and average side-chain saturation in the CNS, kidney, and hepatopancreas. Different organs are shown in different columns, while the two main classes, ether phosphatidylcholines (Ether PC) and phosphatidylcholines (PC) are shown in different rows, in individual subplots; see grey strips for organs and lipid classes. The vertical lines in each plot separate features with decreasing and increasing abundance. Saturation levels denote the average double bond number per side-chain, as follows: PUFA, $n \geq 2$; UNSAT, $2 > n > 0$; SAT, $n = 0$.

homeostasis in mollusks, affecting both chain length and saturation – although these effects are tissue- and lipid class-specific. Particularly, a consistent reduction in the proportion of polyunsaturated fatty acids and a shift toward more saturated fatty acids are revealed by the previous and present findings. These changes are most pronounced in the digestive gland, most likely due to its high metabolic and detoxification activity. Such alterations in lipid homeostasis can reduce membrane fluidity, disrupt signal transduction, and weaken antioxidant defense mechanisms, thereby adversely affecting molluscan physiology. Our study extends our knowledge on mollusks by providing tissue-specific, lipid class-specific changes via untargeted lipidomics, and so highlighting the complexity and organ specificity of lipid responses to TBT exposure. In addition to studies on mollusks, TBT was also shown to alter the amount of storage lipids and lipid composition of *Daphnia* (Jafari et al., 2023; Jordao et al., 2015; Jordao et al., 2016; Moro et al., 2024). Future studies should aim to investigate lipid metabolic pathways and functions more deeply in other invertebrate model animals.

3.4. Changes in the expression of Lym-HSD17B12

In vertebrates, the main function of some HSD17B isozymes is the synthesis of androgens and estrogens, while other HSD17Bs play key roles in other metabolic processes (reviewed by Marchais-Oberwinkler et al., 2011; Prehn et al., 2009; Saloniemi et al., 2012). Among these enzymes, HSD17B12 is known to be essential for fatty acid synthesis and lipid metabolism in mice (Heikelä et al., 2020). In an earlier study, the inhibitory effect of TBT was reported on the enzymatic activity of HSD17Bs in pig (Ohno et al., 2005). Moreover, a later study demonstrated that the expression of HSD17B12 was decreased in the digestive gland of *N. lapillus* following chronic exposure of TBT at 100 ng L^{-1}, suggesting an evolutionary conserved function for this enzyme and pointing out its potential role in TBT-evoked metabolic disruption (Lima et al., 2013).

Using nucleotide sequencing and *in silico* searches, the sequence of Lym-HSD17B12 was identified (**Supplementary Figure 4**) in order to provide further insights into the evolution of HSD17B enzymes and to be able to investigate the alterations in its expression after chronic TBT exposure. The subsequent bioinformatic analyses, including conserved domain analysis (**Supplementary Figure 5**), conservation analysis (**Supplementary Figure 6**), Ribbon diagram prediction (**Supplementary Figure 7**), and phylogenetic analysis (**Supplementary Figure 8**), confirmed that the protein product of the obtained sequence is a *bona fide* HSD17B12 candidate. Our RT-PCR analysis revealed that Lym-HSD17B12 transcript was present in all tissues investigated: CNS, heart, kidney, and hepatopancreas (**Supplementary Figure 9**). This ubiquitous expression corresponds to that reported in *N. lapillus* (Lima et al., 2013) and different vertebrate species (Blanchard and Luu-The, 2007; Heikelä et al., 2020; Moon and Horton, 2003; Sakurai et al., 2006). Similar to the expression of HSD17B12 in *N. lapillus*, the highest expression was detected in the kidney and hepatopancreas (organs with high metabolic rate). Since the current view is that a sex steroid biosynthetic pathway similar to that described in vertebrates is not present in mollusks (Fodor and Pirger, 2022; Markov et al., 2017; Scott, 2012), our results support the idea that in mollusks, like in mammals, the main function of HSD17B12 is the participation in lipid metabolism.

The changes in the expression of Lym-HSD17B12 after the 21-day TBT exposure are shown in Fig. 5. Compared to the control, the chronic TBT exposure caused a 62.6% reduction in Lym-HSD17B12 expression in the CNS (Mann Whitney: $Z = 3.72$, $p < 0.001$) (Fig. 5**A**), a 69.2% reduction in the kidney ($t_{22} = 4.72$, $p < 0.001$) (Fig. 5**B**), and a 74.3% reduction in the hepatopancreas ($t_{22} = 7.44$, $p < 0.001$) (Fig. 5**C**). The decreased expression of Lym-HSD17B12 in the hepatopancreas was the same as that previously described in *N. lapillus* (Lima et al., 2013). TBT was previously shown to modulate the transcription of key elements of lipid metabolism in *Daphnia* (Moro et al., 2024) as well as in different tissues of zebrafish and mice (Grun et al., 2006; Lyssimachou et al., 2015). Our results also demonstrated that application of TBT decreased the expression of HSD17B12 not only in the hepatopancreas but also in the CNS and kidney. Importantly, our findings obtained at the molecular level correlate well with the altered lipid composition revealed at the cellular level, further suggesting that HSD17B12 enzyme is involved in the lipid metabolism and in the TBT-induced metabolic disruption in mollusks. To get a deeper understating of TBT-evoked disruption of lipid homeostasis in *Lymnaea* (and in mollusks in general) at the molecular level, further studies should aim at identifying a wide range of lipogenic genes (e.g. SREBP1) and analyzing their expression after chronic TBT treatments.

4. Conclusions

In summary, our results show that TBT affects the adult specimens of the great pond snail, *Lymnaea* stagnalis from the behavioral to the molecular level at an average environmentally relevant concentration (100 ng L^{-1}). Our results are the first to demonstrate that direct application of TBT alters adult feeding activity of a molluscan species, supporting previous studies on mollusks and flatworms that indicate TBT exerts an

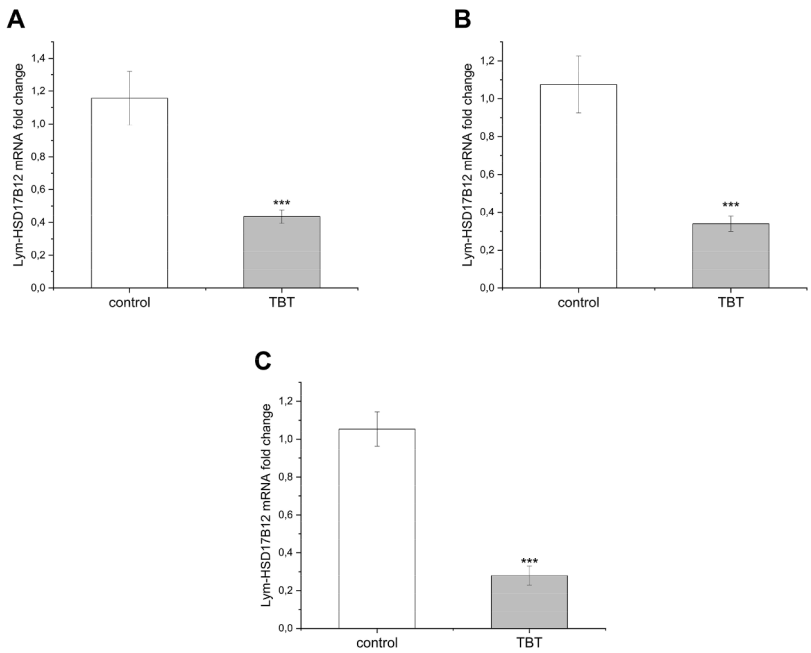

Fig. 5. Expression of Lym-HSD17B12 in the CNS (**A**), kidney (**B**), and hepatopancreas (**C**) after the 21-day TBT exposure. The expression of Lym-HSD17B12 significantly decreased in all tissues investigated after TBT treatment. Each bar represents mean ± SEM (n = 12 animals/group). White columns represent the control, while grey columns represent the treated groups. Significance of differences to the control is indicated by asterisks (***$p < 0.001$).

opposite effect on feeding of invertebrates compared to vertebrates. It is also ascertainable that feeding activity is an excellent target for investigating the effects of TBT pollution in aquatic species. At the histochemical level, the presence and distribution of tin was demonstrated for the first time in an adult molluscan species after chronic TBT exposure, and evidence was provided that TBT induces an increased lysosomal activity in different peripheral tissues.

Our findings also demonstrated that TBT can directly alter the lipid composition in *Lymnaea*, confirming that this compound is not only an endocrine but also a metabolic disruptor in invertebrates. Along with the findings of previous studies on mollusks, our study highlights a consistent reduction in the proportion of PUFA and a shift toward more saturated lipids, suggesting changes in membrane fluidity and signaling capacity. Moreover, our study extends the findings of the previous studies by providing tissue-specific and lipid class-specific changes highlighting the complexity and organ specificity of lipid responses to TBT exposure. Our results confirm that HSD17B12 enzyme plays a key role in lipid metabolism in mollusks (indicating an evolutionarily conserved function) and suggest that it is likely involved in TBT-induced metabolic disruption. We propose that the changes in the lipid homeostasis is a result of an interplay between direct molecular disruption of lipid metabolic pathways (e.g., decreased HSD17B12 expression) and indirect metabolic consequences stemming from nutritional stress (due to the reduced feeding activity and body weight loss). The reduction in PUFA content and chain length suggests an inhibition of elongase or desaturase activity, which is supported by the decreased expression of HSD17B12. Additionally, nutritional stress is known to alter lipid metabolism. Namely, under reduced food intake, many animals mobilize storage lipids (typically long-chain PUFA) and shift toward shorter or more saturated fatty acids.

Although TBT at the low concentrations is not lethal for mollusks, it is clear that it has a strong impact on their physiology and metabolism. Further studies should aim at revealing the exact neuronal background of the altered feeding behavior evoked by TBT, and identifying further molecular elements (e.g., lipogenic genes) involved in the disturbed lipid homeostasis.

Ethics statement

All procedures, methods, and experiments on the specimens were carried out in accordance with the relevant guidelines and regulations approved by the Scientific Committee of Animal Experimentation of the Balaton Limnological Research Institute (VE-I-001/01890-10/2013).

Funding

This work was supported by the Bolyai Foundation (#BO/00521/24, I.F.; #BO/00215/23, S.G.), the National Brain Project (#NAP2022-I-10/2022; Z.P.), the Hungarian Scientific Research Fund (#138039; Z.P.; #146787, I.F.), the National Laboratory for Water Science and Water Security (#RRF 2.3.1-21-2022-00008, HUN-REN BLRI), the Sustainable Development and Technologies National Programme of the Hungarian Academy of Sciences (#NP2022-II3/2022; HUN-REN BLRI), the Thematic Excellence Program (#TKP2021-EGA-17, J.S.), and the New National Excellence Program of the Ministry for Innovation and Technology from the source of the National Research, Development and Innovation Fund (ÚNKP-23-4-II-PE-1; R.S.).

CRediT authorship contribution statement

István Fodor: Writing – original draft, Visualization, Methodology, Investigation, Funding acquisition, Data curation, Conceptualization. **János Schmidt:** Writing – review & editing, Methodology, Investigation, Funding acquisition, Data curation. **Réka Svigruha:** Writing – review & editing, Investigation, Funding acquisition. **Zita László:** Investigation. **László Molnár:** Writing – review & editing, Visualization, Methodology, Investigation. **Sándor Gonda:** Data curation, Funding acquisition, Visualization, Writing – review & editing. **Károly Elekes:** Writing – review & editing. **Zsolt Pirger:** Writing – review & editing, Investigation, Funding acquisition.

Declaration of competing interest

The authors declare that they have no known competing financial interests or personal relationships that could have appeared to influence

the work reported in this paper.

Acknowledgement

The authors thank some of the attendees, especially Anna Padányi, of the International Neuroscience Conference 2024 (Pécs, Hungary) for providing constructive comments and ideas for this work. The authors also thank Bence Kiss (Department of Biochemistry and Medical Chemistry, University of Pécs, Hungary) for making the Ribbon diagram of *Lymnaea* HSD17B12 protein. Open access funding was provided by the Hungarian Research Network (HUN-REN).

Supplementary materials

Supplementary material associated with this article can be found, in the online version, at doi:10.1016/j.aquatox.2025.107404.

Data availability

Data will be made available on request.

References

Ali, H., Ali, S., Mazhar, M., Ali, A., Jahan, A., Ali, A., 2017. Eosin fluorescence: A diagnostic tool for quantification of liver injury. Photodiagnosis. Photodyn. Ther. 19, 37–44. https://doi.org/10.1016/j.pdpdt.2017.03.016.

Amorim, J., Abreu, I., Rodrigues, P., Peixoto, D., Pinheiro, C., Saraiva, A., Carvalho, A.P., Guimaraes, L., Oliva-Teles, L., 2019. *Lymnaea stagnalis* as a freshwater model invertebrate for ecotoxicological studies. Sci. Total Environ. 669, 11–28. https://doi.org/10.1016/j.scitotenv.2019.03.035.

Antizar-Ladislao, B., 2008. Environmental levels, toxicity and human exposure to tributyltin (TBT)-contaminated marine environment. a review. Environ. Int. 34, 292–308. https://doi.org/10.1016/j.envint.2007.09.005.

Bandow, C., Weltje, L., 2012. Development of an embryo toxicity test with the pond snail *Lymnaea stagnalis* using the model substance tributyltin and common solvents. Sci. Total Environ. 435-436, 90–95. https://doi.org/10.1016/j.scitotenv.2012.07.005.

Barbos, M.A.G., Capela, R., Rodolfo, J., Fonseca, E., Montes, R., André, A., Capitao, A., Carvalho, A.P., Quintana, J.B., Castro, L.F.C., et al., 2019. Linking chemical exposure to lipid homeostasis: A municipal waste water treatment plant influent is obesogenic for zebrafish larvae. Ecotox. Environ. Saf. 182, 109406. https://doi.org/10.1016/j.ecoenv.2019.109406.

Batabyal, A., Rivi, V., Benatti, C., Blom, J.M.C., Tascedda, F., Lukowiak, K., 2024. Snails go on a fast when acetylsalicylic acid comes along with heat stress: A possible effect of HSPs and serotonergic system on the feeding response. Comp. Biochem. Physiol. C Toxicol. Pharmacol. 276, 109805. https://doi.org/10.1016/j.cbpc.2023.109805.

Benjamin, P.R., Crossley, M., 2020. Gastropod feeding systems: evolution of neural circuits that generate diverse behaviors. Oxford Research Encyclopedia of Neuroscience. https://doi.org/10.1093/acrefore/9780190264086.013.186.

Beyer, J., Song, Y., Tollefsen, K.E., Berge, J.A., Tveiten, L., Helland, A., Oxnevad, S., Schoyen, M., 2022. The ecotoxicology of marine tributyltin (TBT) hotspots: A review. Mar. Environ. Res. 179, 105689. https://doi.org/10.1016/j.marenvres.2022.105689.

Bisong, E., 2019. Building Machine Learning and Deep Learning Models on Google Cloud Platform: A Comprehensive Guide for Beginners. Apress.

Blanchard, P.G., Luu-The, V., 2007. Differential androgen and estrogen substrates specificity in the mouse and primates type 12 17beta-hydroxysteroid dehydrogenase. J. Endocrinol. 194, 449–455. https://doi.org/10.1677/JOE-07-0144.

Bligh, E.G., Dyer, W.J., 1959. A rapid method of total lipid extraction and purification. Can. J. Biochem. Physiol. 37, 911–917. https://doi.org/10.1139/o59-099.

Bo, E., Farinetti, A., Marraudino, M., Sterchele, D., Eva, C., Gotti, S., Panzica, G., 2016. Adult exposure to tributyltin affects hypothalamic neuropeptide Y, Y1 receptor distribution, and circulating leptin in mice. Andrology 4, 723–734. https://doi.org/10.1111/andr.12222.

Capitao, A., Lopes-Marques, M., Páscoa, I., Ruivo, R., Mendiratta, N., Fonseca, E., Castro, L.F.C., Santos, M.M., 2020. The Echinodermata PPAR: Functional characterization and exploitation by the model lipid homeostasis regulator tributyltin. Environ. Pollut. 263, 114467. https://doi.org/10.1016/j.envpol.2020.114467.

Capitao, A.M.F., Lopes-Marques, M., Páscoa, I., Sainath, S.B., Hiromori, Y., Matsumaru, D., Nakanishi, T., Ruivo, R., Santos, M.M., Castro, L.F.C., 2021. An ancestral nuclear receptor couple, PPAR-RXR, is exploited by organotins. Sci. Total Environ. 797, 149044. https://doi.org/10.1016/j.scitotenv.2021.149044.

Castro, L.F., Lima, D., Machado, A., Melo, C., Hiromori, Y., Nishikawa, J., Nakanishi, T., Reis-Henriques, M.A., Santos, M.M., 2007. Imposex induction is mediated through the Retinoid X Receptor signalling pathway in the neogastropod *Nucella lapillus*. Aquat. Toxicol. 85, 57–66. https://doi.org/10.1016/j.aquatox.2007.07.016.

Champeau, O., Narbonne, J.F.S., 2006. Effects of tributyltin and 17β-estradiol on immune and lysosomal systems of the Asian clam *Corbicula fluminea* (M.). Environ. Toxicol. Pharmacol. 21, 323–330. https://doi.org/10.1016/j.etap.2005.10.007.

Chen, H.G., Jia, X.P., Cai, W.G., Lin, Q., Ma, S.W., 2011. Antioxidant Responses and Bioaccumulation in Green-lipped Mussels (*Perna viridis*) Under Acute Tributyltin Chloride Exposure. Bull. Environ. Contam. Toxicol. 87, 506–511. https://doi.org/10.1007/s00128-011-0390-0.

Czech, P., Weber, K., Dietrich, D.R., 2001. Effects of endocrine modulating substances on reproduction in the hermaphroditic snail *Lymnaea stagnalis* L. Aquat Toxicol 53, 103–114. https://doi.org/10.1016/s0166-445x(00)00169-7.

Desouky, M.M., 2006. Tissue distribution and subcellular localization of trace metals in the pond snail *Lymnaea stagnalis* with special reference to the role of lysosomal granules in metal sequestration. Aquat. Toxicol. 77, 143–152. https://doi.org/10.1016/j.aquatox.2005.11.009.

Elangovan, R., McCrohan, C.R., Ballance, S., Powell, J.J., White, K.N., 2000. Localization and fate of aluminium in the digestive gland of the freshwater snail *Lymnaea stagnalis*. Tissue & Cell 32, 79–87. https://doi.org/10.1054/tice.1999.0089.

Essawy, A.E., El-Sherief, S.S., Sadek, I.A., Soffar, A.A., 2011. Neuropathological Effect of Tributyltin on the Cerebral Ganglia of the Land Snail, *Eobania vermiculata*. Int. J. Zool. Res. 7, 252–262. https://doi.org/10.3923/ijzr.2011.252.262.

Farinetti, A., Marraudino, M., Ponti, G., Panzica, G., Gotti, S., 2018. Chronic treatment with tributyltin induces sexually dimorphic alterations in the hypothalamic POMC system of adult mice. Cell Tissue Res 374, 587–594. https://doi.org/10.1007/s00441-018-2896-9.

Fent, K., Meier, W., 1992. Tributyltin-Induced Effects on Early Life Stages of Minnows *Phoxinus phoxinus*. Arch. Environ. Contam. Toxicol. 22, 428–438. https://doi.org/10.1007/Bf00212563.

Fodor, I., Hussein, A.A., Benjamin, P.R., Koene, J.M., Pirger, Z., 2020. The unlimited potential of the great pond snail, *Lymnaea stagnalis*. eLife 9, e56962. https://doi.org/10.7554/eLife.56962.

Fodor, I., Svigruha, R., Bozso, Z., Toth, G.K., Osugi, T., Yamamoto, T., Satake, H., Pirger, Z., 2021. Functional characterization and related evolutionary implications of invertebrate gonadotropin-releasing hormone/corazonin in a well-established model species. Sci. Rep. 11, 10028. https://doi.org/10.1038/s41598-021-89614-5.

Fodor, I., Pirger, Z., 2022. From dark to light - an overview of over 70 years of endocrine disruption research on marine mollusks. Front. Endocrinol. 13, 903575. https://doi.org/10.3389/fendo.2022.903575.

Geyer, G., 1973. Ultrahistochemie. Histochemische Arbeitsvorschriften für die Elektronenmikroskopie. VEB G. Fischer, Jena.

Giusti, A., Leprince, P., Mazzucchelli, G., Thome, J.P., Lagadic, L., Ducrot, V., Joaquim-Justo, C., 2013a. Proteomic analysis of the reproductive organs of the hermaphroditic gastropod *Lymnaea stagnalis* exposed to different endocrine disrupting chemicals. PLoS One 8, e81086. https://doi.org/10.1371/journal.pone.0081086.

Giusti, A., Barsi, A., Dugue, M., Collinet, M., Thome, J.P., Joaquim-Justo, C., Roig, B., Lagadic, L., Ducrot, V., 2013b. Reproductive impacts of tributyltin (TBT) and triphenyltin (TPT) in the hermaphroditic freshwater gastropod *Lymnaea stagnalis*. Environ. Toxicol. Chem. 32, 1552–1560. https://doi.org/10.1002/etc.2200.

Giusti, A., Ducrot, V., Joaquim-Justo, C., Lagadic, L., 2013c. Testosterone levels and fecundity in the hermaphroditic aquatic snail *Lymnaea stagnalis* exposed to testosterone and endocrine disruptors. Environ. Toxicol. Chem. 32, 1740–1745. https://doi.org/10.1002/etc.2234.

Graceli, J.B., Sena, G.C., Lopes, P.F.I., Zamprogno, G.C., da Costa, M.B., Godoi, A.F.L., dos Santos, D.M., de Marchi, M.R.R., Fernandez, M.A.D., 2013. Organotins: A review of their reproductive toxicity, biochemistry, and environmental fate. Reprod. Toxicol. 36, 40–52. https://doi.org/10.1016/j.reprotox.2012.11.008.

Grun, F., Watanabe, H., Zamanian, Z., Maeda, L., Arima, K., Cubacha, R., Gardiner, D.M., Kanno, J., Iguchi, T., Blumberg, B., 2006. Endocrine-disrupting organotin compounds are potent inducers of adipogenesis in vertebrates. Mol. Endocrinol. 20, 2141–2155. https://doi.org/10.1210/me.2005-0367.

Guex, N., Peitsch, M.C., 1997. SWISS-MODEL and the Swiss-PdbViewer: an environment for comparative protein modeling. Electrophoresis 18, 2714–2723. https://doi.org/10.1002/elps.1150181505.

Heikelä, H., Ruohonen, S.T., Adam, M., Viitanen, R., Liljenbäck, H., Eskola, O., Gabriel, M., Mairinoja, L., Pessia, A., Velagapudi, V., et al., 2020. Hydroxysteroid (17β) dehydrogenase 12 is essential for metabolic homeostasis in adult mice. Am. J. Physiol. Endocrinol. Metab. 319, E494–E508. https://doi.org/10.1152/ajpendo.00042.2020.

Herwig, H.J., Holwerda, D.A., 1986. Cytochemical localization of tin in freshwater mussels exposed to di-n-butyltin dichloride. Aquat. Toxicol. 9, 117–128. https://doi.org/10.1016/0166-445X(86)90018-4.

Horiguchi, T., Ohta, Y., Nishikawa, T., Shiraishi, F., Shiraishi, H., Morita, M., 2008. Exposure to 9-cis retinoic acid induces penis and vas deferens development in the female rock shell, *Thais clavigera*. Cell. Biol. Toxicol. 24, 553–562. https://doi.org/10.1007/s10565-007-9051-9.

Horiguchi, T., Ohta, Y., 2020. A Critical Review of Sex Steroid Hormones and the Induction Mechanisms of Imposex in Gastropod Mollusks. In: Saber Saleuddin, A.B. L., Orchard, Ian (Eds.), Advances in Invertebrate (Neuro)Endocrinology. Apple Academic Press, Boca Raton.

Inoue, S., Oshima, Y., Nagai, K., Yamamoto, T., Go, J., Kai, N., Honjo, T., 2004. Effect of maternal exposure to tributyltin on reproduction of the pearl oyster (*Pinctada fucata martensii*). Environ. Toxicol. Chem. 23, 1276–1281. https://doi.org/10.1897/03-265.

Inoue, S., Oshima, Y., Usuki, H., Hamaguchi, M., Hanamura, Y., Kai, N., Shimasaki, Y., Honjo, T., 2006. Effects of tributyltin maternal and/or waterborne exposure on the embryonic development of the Manila clam, *Ruditapes philippinarum*. Chemosphere 63, 881–888. https://doi.org/10.1016/j.chemosphere.2005.07.047.

Iyapparaj, P., Revathi, P., Ramasubburayan, R., Prakash, S., Anantharaman, P., Immanuel, G., Palavesam, A., 2013. Antifouling activity of the methanolic extract of

Syringodium isoetifolium, and its toxicity relative to tributyltin on the ovarian development of brown mussel *Perna indica*. Ecotoxicol. Environ. Saf. 89, 231–238. https://doi.org/10.1016/j.ecoenv.2012.12.001.

Jafari, J.M., Casas, J., Barata, C., Abdollahi, H., Tauler, R., 2023. Non-target ROIMCR LC-MS analysis of the disruptive effects of TBT over time on the lipidomics of *Daphnia magna*. Metabolomics 19, 70. https://doi.org/10.1007/s11306-023-02030-w.

Janer, G., Navarro, J.C., Porte, C., 2007. Exposure to TBT increases accumulation of lipids and alters fatty acid homeostasis in the ramshorn snail *Marisa cornuarietis*. Comp. Biochem. Physiol. C Toxicol. Pharmacol. 146, 368–374. https://doi.org/10.1016/j.cbpc.2007.04.009.

Jiang, M.W., Zhang, Z.H., Han, Q.X., Peng, R.B., Shi, H.L., Jiang, X.M., 2023. Embryonic exposure to environmentally relevant levels of tributyltin affects embryonic tributyltin bioaccumulation and the physiological responses of juveniles in cuttlefish. Ecotoxicol.Environ. Safety. 256, 114894. https://doi.org/10.1016/j.ecoenv.2023.114894.

Jordao, R., Casas, J., Fabrias, G., Campos, B., Piña, B., Lemos, M.F.L., Soares, A.M.V.M., Tauler, R., Barata, C., 2015. Obesogens beyond Vertebrates: Lipid Perturbation by Tributyltin in the Crustacean *Dahpnia magna*. Environ. Health Perspect. 123, 813–819. https://doi.org/10.1289/ehp.1409163.

Jordão, R., Campos, B., Piña, B., Tauler, R., Soares, A.M., Barata, C., 2016. Mechanisms of Action of Compounds That Enhance Storage Lipid Accumulation in *Daphnia magna*. Environ. Sci. Technol. 50, 13565–13573. https://doi.org/10.1021/acs.est.6b04768.

Jumper, J., Evans, R., Pritzel, A., Green, T., Figurnov, M., Ronneberger, O., Tunyasuvunakool, K., Bates, R., Zidek, A., Potapenko, A., et al., 2021. Highly accurate protein structure prediction with AlphaFold. Nature 596, 583–589. https://doi.org/10.1038/s41586-021-03819-2.

Kishimoto, K., Matsuo, S.I., Kanemoto, Y., Ishibashi, H., Oyama, Y., Akaike, N., 2001. Nanomolar concentrations of tri-n-butyltin facilitate γ-aminobutyric acidergic synaptic transmission in rat hypothalamic neurons. J. Pharmacol. Exp. Ther. 299, 171–177.

Kopp, R., Martínez, I.O., Legradi, J., Legler, J., 2017. Exposure to endocrine disrupting chemicals perturbs lipid metabolism and circadian rhythms. J. Environ. Sci. 62, 133–137. https://doi.org/10.1016/j.jes.2017.10.013.

Kumar, S., Stecher, G., Tamura, K., 2016. MEGA7: Molecular Evolutionary Genetics Analysis Version 7.0 for Bigger Datasets. Mol. Biol. Evol. 33, 1870–1874. https://doi.org/10.1093/molbev/msw054.

Lagadic, L., Katsiadaki, I., Biever, R., Guiney, P.D., Karouna-Renier, N., Schwarz, T., Meador, J.P., 2018. Tributyltin: Advancing the Science on Assessing Endocrine Disruption with an Unconventional Endocrine-Disrupting Compound. Rev. Environ. Contam. Toxicol. 245, 65–127. https://doi.org/10.1007/398_2017_8.

Leung, K.M.Y., Grist, E.P.M., Morley, N.J., Morritt, D., Crane, M., 2007. Chronic toxicity of tributyltin to development and reproduction of the European freshwater snail *Lymnaea stagnalis* (L.). Chemosphere 66, 1358–1366. https://doi.org/10.1016/j.chemosphere.2006.06.051.

Li, P., Li, Z.H., 2021. Neurotoxicity and physiological stress in brain of zebrafish chronically exposed to tributyltin. J. Toxicol. Environ. Health A. 84, 20–30. https://doi.org/10.1080/15287394.2020.1828209.

Liang, X.F., Souders, C.L., Zhang, J.L., Martyniuk, C.J., 2017. Tributyltin induces premature hatching and reduces locomotor activity in zebrafish (*Danio rerio*) embryos/larvae at environmentally relevant levels. Chemosphere 189, 498–506. https://doi.org/10.1016/j.chemosphere.2017.09.093.

Lima, D., Reis-Henriques, M.A., Silva, R., Santos, A.I., Castro, L.F., Santos, M.M., 2011. Tributyltin-induced imposex in marine gastropods involves tissue-specific modulation of the retinoid X receptor. Aquat. Toxicol. 101, 221–227. https://doi.org/10.1016/j.aquatox.2010.09.022.

Lima, D., Machado, A., Reis-Henriques, M.A., Rocha, E., Santos, M.M., Castro, L.F., 2013. Cloning and expression analysis of the 17beta hydroxysteroid dehydrogenase type 12 (HSD17B12) in the neogastropod *Nucella lapillus*. J. Steroid. Biochem. Mol. Biol. 134, 8–14. https://doi.org/10.1016/j.jsbmb.2012.10.005.

Lu, S., Wang, J., Chitsaz, F., Derbyshire, M.K., Geer, R.C., Gonzales, N.R., Gwadz, M., Hurwitz, D.I., Marchler, G.H., Song, J.S., et al., 2020. CDD/SPARCLE: the conserved domain database in 2020. Nucleic Acids Res 48, D265–D268. https://doi.org/10.1093/nar/gkz991.

Lyssimachou, A., Navarro, J.C., Bachmann, J., Porte, C., 2009. Triphenyltin alters lipid homeostasis in females of the ramshorn snail *Marisa cornuarietis*. Environ. Pollut. 157, 1714–1720. https://doi.org/10.1016/j.envpol.2008.12.013.

Lyssimachou, A., Santos, J.G., André, A., Soares, J., Lima, D., Guimaraes, L., Almeida, C. M.R., Teixeira, C., Castro, L.F.C., Santos, M.M., 2015. The Mammalian "Obesogen" Tributyltin Targets Hepatic Triglyceride Accumulation and the Transcriptional Regulation of Lipid Metabolism in the Liver and Brain of Zebrafish. Plos One. 10, e0143911. https://doi.org/10.1371/journal.pone.0143911.

Marchais-Oberwinkler, S., Henn, C., Moller, G., Klein, T., Negri, M., Oster, A., Spadaro, A., Werth, R., Wetzel, M., Xu, K., et al., 2011. 17beta-Hydroxysteroid dehydrogenases (17beta-HSDs) as therapeutic targets: protein structures, functions, and recent progress in inhibitor development. J. Steroid. Biochem. Mol. Biol. 125, 66–82. https://doi.org/10.1016/j.jsbmb.2010.12.013.

Marchler-Bauer, A., Bo, Y., Han, L., He, J., Lanczycki, C.J., Lu, S., Chitsaz, F., Derbyshire, M.K., Geer, R.C., Gonzales, N.R., et al., 2017. CDD/SPARCLE: functional classification of proteins via subfamily domain architectures. Nucleic Acids Res 45, D200–D203. https://doi.org/10.1093/nar/gkw1129.

Markov, G.V., Gutierreze-Mazariegos, J., Pitrat, D., Billas, I.M.L., Bonneton, F., Moras, D., Hasserodt, J., Lecointre, G., Laudet, V., 2017. Origin of an ancient hormone/receptor couple revealed by resurrection of an ancestral estrogen. Sci. Adv. 3, e1601778. https://doi.org/10.1126/sciadv.1601778.

Martínez, M.L., Piol, M.N., Nudelman, N.S., Guerrero, N.R.V., 2017. Tributyltin bioaccumulation and toxic effects in freshwater gastropods *Pomacea canaliculata* after a chronic exposure: field and laboratory studies. Ecotoxicology 26, 691–701. https://doi.org/10.1007/s10646-017-1801-8.

Metelkova, L., Zhakovskaya, Z., Kukhareva, G., Voskoboinikov, G., Zimina, O., 2022. Organotin compounds (OTs) in surface sediments, bivalves and algae from the Russian coast of the Barents Sea (Kola Peninsula) and the Fram Strait (Svalbard Archipelago). Environ. Sci. Pollut. Res. Int. 29, 34659–34669. https://doi.org/10.1007/s11356-021-18091-0.

Mitra, S., Gera, R., Siddiqui, W.A., Khandelwal, S., 2013. Tributyltin induces oxidative damage, inflammation and apoptosis via disturbance in blood-brain barrier and metal homeostasis in cerebral cortex of rat brain: an *in vivo* and *in vitro* study. Toxicology 310, 39–52. https://doi.org/10.1016/j.tox.2013.05.011.

Mohamed, A., Jeffrey, M., 2023. lipidr: Data Mining and Analysis of Lipidomics Datasets. Bioconductor Repositroy. https://doi.org/10.18129/B9.bioc.lipidr. R package version 2.16.0. https://git.bioconductor.org/packages/lipidr.

Moon, Y.A., Horton, J.D., 2003. Identification of two mammalian reductases involved in the two-carbon fatty acyl elongation cascade. J. Biol. Chem. 278, 7335–7343. https://doi.org/10.1074/jbc.M211684200.

Moro, H., Raldúa, D., Barata, C., 2024. Developmental defects in cognition, metabolic and cardiac function following maternal exposures to low environmental levels of selective serotonin re-uptake inhibitors and tributyltin in *Daphnia magna*. Sci. Total Environ. 917, 170463. https://doi.org/10.1016/j.scitotenv.2024.170463.

Nishikawa, J., Mamiya, S., Kanayama, T., Nishikawa, T., Shiraishi, F., Horiguchi, T., 2004. Involvement of the retinoid X receptor in the development of imposex caused by organotins in gastropods. Environ. Sci. Technol. 38, 6271–6276. https://doi.org/10.1021/es049593u.

Ofoegbu, P.U., Simao, F.C.P., Cruz, A., Mendo, S., Soares, A.M.V.M., Pestana, J.L.T., 2016. Toxicity of tributyltin (TBT) to the freshwater planarian *Schmidtea mediterranea*. Chemosphere 148, 61–67. https://doi.org/10.1016/j.chemosphere.2015.12.131.

Ohno, S., Nakajima, Y., Nakajin, S., 2005. Triphenyltin and Tributyltin inhibit pig testicular 17beta-hydroxysteroid dehydrogenase activity and suppress testicular testosterone biosynthesis. Steroids 70, 645–651. https://doi.org/10.1016/j.steroids.2005.03.005.

Ortiz-Villanueva, E., Jaumot, J., Martínez, R., Navarro-Martín, L., Piña, B., Tauler, R., 2018. Assessment of endocrine disruptors effects on zebrafish (*Danio rerio*) embryos by untargeted LC-HRMS metabolomic analysis. Sci. Total Environ. 635, 156–166. https://doi.org/10.1016/j.scitotenv.2018.03.369.

Pirger, Z., László, Z., Naskar, S., Crossley, M., O'Shea, M., Benjamin, P.R., Kemenes, G., Kemenes, I., 2021. Interneuronal mechanisms for learning-induced switch in a sensory response that anticipates changes in behavioral outcomes. Curr. Biol. 31, 1754–1761. https://doi.org/10.1016/j.cub.2021.01.072 e3.

Pirger, Z., Urban, P., Galik, B., Kiss, B., Tapodi, A., Schmidt, J., Toth, G., Koene, J.M., Kemenes, G., Reglodi, D., et al., 2024. Same same, but different: exploring the enigmatic role of the pituitary adenylate cyclase- activating polypeptide (PACAP) in invertebrate physiology. J. Comp. Physiol. A. https://doi.org/10.1007/s00359-024-01706-5.

Ponti, G., Bo, E., Bonaldo, B., Farinetti, A., Marraudino, M., Panzica, G., Gotti, S., 2023. Perinatal exposure to tributyltin affects feeding behavior and expression of hypothalamic neuropeptide Y in the paraventricular nucleus of adult mice. J. Anat. 242, 235–244. https://doi.org/10.1111/joa.13766.

Prehn, C., Moller, G., Adamski, J., 2009. Recent advances in 17beta-hydroxysteroid dehydrogenases. J. Steroid. Biochem. Mol. Biol. 114, 72–77. https://doi.org/10.1016/j.jsbmb.2008.12.024.

Puccia, E., Messina, C.M., Cangialosi, M.V., D'Agati, P., Mansueto, C., Pellerito, C., Nagy, L., Mansueto, V., Scopelliti, M., Fiore, T., et al., 2005. Lipid and fatty acid variations in *Ciona intestinalis* ovary after tri-n-butyltin(IV) chloride exposure. App. Organomet. Chem. 19, 23–29. https://doi.org/10.1002/aoc.765.

PyMOL, 2020. The PyMOL Molecular Graphics System, 2020. Schrödinger, LLC. Version 2.4.0.

Rabitto, I.S., Costa, J.R.M.A., de Assis, H.C.S., Pelletier, É., Akaishi, F.M., Anjos, A., Randi, M.A.F., Ribeiro, C.A.O., 2005. Effects of dietary Pb(II) and tributyltin on neotropical fish, *Hoplias malabaricus*: histopathological and biochemical findings. Ecotoxicol. Environ. Saf. 60, 147–156. https://doi.org/10.1016/j.ecoenv.2004.03.002.

Reátegui-Zirena, E.G., Salice, C.J., 2018. Parental diet affects embryogenesis of the great pond snail (*Lymnaea stagnalis*) exposed to cadmium, pyraclostrobin, and tributyltin. Environ. Toxicol. Chem. 37, 2428–2438. https://doi.org/10.1002/etc.4202.

Rivi, V., Benatti, C., Colliva, C., Radighieri, G., Brunello, N., Tascedda, F., Blom, J.M.C., 2020. *Lymnaea stagnalis* as model for translational neuroscience research: From pond to bench. Neurosci. Biobehav. Rev. 108, 602–616. https://doi.org/10.1016/j.neubiorev.2019.11.020.

Rivi, V., Batabyal, A., Wiley, B., Benatti, C., Tascedda, F., Blom, J.M.C., Lukowiak, K., 2022. Fluoride affects memory by altering the transcriptional activity in the central nervous system of *Lymnaea stagnalis*. Neurotoxicology 92, 61–66. https://doi.org/10.1016/j.neuro.2022.07.007.

Rivi, V., Batabyal, A., Lukowiak, K., Benatti, C., Rigillo, G., Tascedda, F., Blom, J.M.C., 2023. LPS-Induced Garcia Effect and Its Pharmacological Regulation Mediated by Acetylsalicylic Acid: Behavioral and Transcriptional Evidence. Biology (Basel) 12, 1100. https://doi.org/10.3390/biology12081100.

Rodrigues-Pereira, P., Andrade, M.N., Santos-Silva, A.P., Teixeira, M.P., Soares, P., Graceli, J.B., de Carvalho, D.P., Dias, G.R.M., Ferreira, A.C.F., Miranda-Alves, L., 2022. Subacute and low-dose tributyltin exposure disturbs the mammalian hypothalamus-pituitary-thyroid axis in a sex-dependent manner. Comp. Biochem.

Physiol. C Toxicol. Pharmacol. 254, 109279. https://doi.org/10.1016/j.cbpc.2022.109279.

Sadamoto, H., Takahashi, H., Okada, T., Kenmoku, H., Toyota, M., Asakawa, Y., 2012. De novo sequencing and transcriptome analysis of the central nervous system of mollusc *Lymnaea stagnalis* by deep RNA sequencing. PLoS One 7, e42546. https://doi.org/10.1371/journal.pone.0042546.

Sakr, S., Rashad, W., Abaza, M.T., 2021. The ameliorative effect of oleifera oil on tributyltin-induced brain toxicity in albino rats. Environ. Toxicol. 36, 2025–2039. https://doi.org/10.1002/tox.23320.

Sakurai, N., Miki, Y., Suzuki, T., Watanabe, K., Narita, T., Ando, K., Yung, T.M., Aoki, D., Sasano, H., Handa, H., 2006. Systemic distribution and tissue localizations of human 17beta-hydroxysteroid dehydrogenase type 12. J. Steroid. Biochem. Mol. Biol. 99, 174–181. https://doi.org/10.1016/j.jsbmb.2006.01.010.

Saloniemi, T., Jokela, H., Strauss, L., Pakarinen, P., Poutanen, M., 2012. The diversity of sex steroid action: novel functions of hydroxysteroid (17beta) dehydrogenases as revealed by genetically modified mouse models. J. Endocrinol. 212, 27–40. https://doi.org/10.1530/JOE-11-0315.

Scott, A.P., 2012. Do mollusks use vertebrate sex steroids as reproductive hormones? Part I. Critical appraisal of the evidence for the presence, biosynthesis and uptake of steroids. Steroids 77, 1450–1468. https://doi.org/10.1016/j.steroids.2012.08.009.

Scott, A.P., 2013. Do mollusks use vertebrate sex steroids as reproductive hormones? II. Critical review of the evidence that steroids have biological effects. Steroids 78, 268–281. https://doi.org/10.1016/j.steroids.2012.11.006.

Shaban, S.F., Khattab, M.A., Abd El Hameed, S.H., Abdelrahman, S.A., 2023. Evaluating the histomorphological and biochemical changes induced by Tributyltin Chloride on pituitary-testicular axis of adult albino rats and the possible ameliorative role of hesperidin. Ultrastruct. Pathol. 47, 304–323. https://doi.org/10.1080/01913123.2023.2195489.

Sternberg, R.M., Hotchkiss, A.K., Leblanc, G.A., 2008. Synchronized expression of retinoid X receptor mRNA with reproductive tract recrudescence in an imposex-susceptible mollusc. Environ. Sci. Technol. 42, 1345–1351. https://doi.org/10.1021/es702381g.

Svigruha, R., Fodor, I., Padisak, J., Pirger, Z., 2021. Progestogen-induced alterations and their ecological relevance in different embryonic and adult behaviours of an invertebrate model species, the great pond snail (*Lymnaea stagnalis*). Environ. Sci. Pollut. Res. Int. 28, 59391–59402. https://doi.org/10.1007/s11356-020-12094-z.

Svigruha, R., Molnár, L., Elekes, K., Pirger, Z., Fodor, I., 2024. Effect of tributyltin exposure on the embryonic development and behavior of a molluscan model species, *Lymnaea stagnalis*. Comp Biochem Physiol C Toxicol Pharmacol 285, 109996. https://doi.org/10.1016/j.cbpc.2024.109996.

R Core Team, 2025. R: A language and environment for statistical computing.

Triebskorn, R., Kohler, H.R., Flemming, J., Braunbeck, T., Negele, R.D., Rahmann, H., 1994. Evaluation of Bis(Tri-N-Butyltin)Oxide (TBTO) Neurotoxicity in Rainbow-Trout (*Oncorhynchus mykiss*). I. Behavior, Weight Increase, and Tin Content. Aquat. Toxicol. 30, 189–197. https://doi.org/10.1016/0166-445x(94)90057-4.

Tsugawa, H., Ikeda, K., Takahashi, M., Satoh, A., Mori, Y., Uchino, H., Okahashi, N., Yamada, Y., Tada, I., Bonini, P., et al., 2020. A lipidome atlas in MS-DIAL 4. Nat. Biotechnol. 38, 1159. https://doi.org/10.1038/s41587-020-0531-2. -+.

Uc-Peraza, R.G., Castro, I.B., Fillmann, G., 2022. An absurd scenario in 2021: Banned TBT-based antifouling products still available on the market. Sci. Total Environ. 805, 150377. https://doi.org/10.1016/j.scitotenv.2021.150377.

Waheed, A.A., Rao, K.S., Gupta, P.D., 2000. Mechanism of dye binding in the protein assay using eosin dyes. Anal. Biochem. 287, 73–79. https://doi.org/10.1006/abio.2000.4793.

Wang, X.H., Fang, C., Hong, H.S., Wang, W.X., 2010. Gender differences in TBT accumulation and transformation in *Thais clavigera* after aqueous and dietary exposure. Aquat. Toxicol. 99, 413–422. https://doi.org/10.1016/j.aquatox.2010.06.001.

Yu, A., Wang, X.L., Zuo, Z.H., Cai, J.L., Wang, C.G., 2013. Tributyltin exposure influences predatory behavior, neurotransmitter content and receptor expression in *Sebastiscus marmoratus*. Aquat. Toxicol. 128, 158–162. https://doi.org/10.1016/j.aquatox.2012.12.008.

Zhang, J., Sun, P., Yang, F., Kong, T., Zhang, R., 2016. Tributyltin disrupts feeding and energy metabolism in the goldfish (*Carassius auratus*). Chemosphere 152, 221–228. https://doi.org/10.1016/j.chemosphere.2016.02.127.

Zhou, J., Zhu, X.S., Cai, Z.H., 2010. Tributyltin toxicity in abalone (*Haliotis diversicolor supertexta*) assessed by antioxidant enzyme activity, metabolic response, and histopathology. J. Hazard. Mater. 183, 428–433. https://doi.org/10.1016/j.jhazmat.2010.07.042.

Zuo, Z.H., Chen, S.Z., Wu, T.A., Zhang, J.L., Su, Y., Chen, Y.X., Wang, C.G., 2011. Tributyltin Causes Obesity and Hepatic Steatosis in Male Mice. Environ. Toxicol. 26, 79–85. https://doi.org/10.1002/tox.20531.